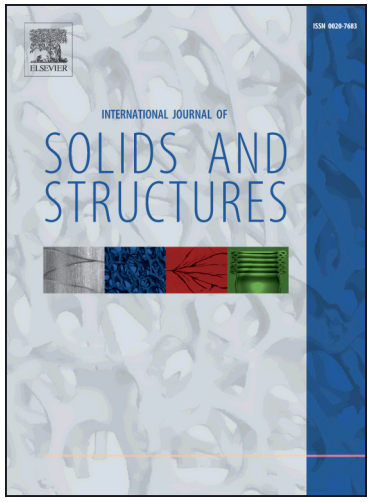

Effective insights into the geometric stability of symmetric skeletal structures under symmetric variations

Yao Chen, Pooya Sareh, Jian Feng

PII: S0020-7683(15)00241-3
DOI: http://dx.doi.org/10.1016/j.ijsolstr.2015.05.023
Reference: SAS 8788

To appear in: *International Journal of Solids and Structures*

Received Date: 16 December 2014
Revised Date: 15 May 2015

Please cite this article as: Chen, Y., Sareh, P., Feng, J., Effective insights into the geometric stability of symmetric skeletal structures under symmetric variations, *International Journal of Solids and Structures* (2015), doi: http://dx.doi.org/10.1016/j.ijsolstr.2015.05.023

Effective insights into the geometric stability of symmetric skeletal structures under symmetric variations

Yao Chen[a], Pooya Sareh[b], Jian Feng[a*]

[a] Key Laboratory of Concrete and Prestressed Concrete Structures of Ministry of Education, Southeast University; National Prestress Engineering Research Center, Southeast University, Nanjing 210096, China

[b] Advanced Structures group, Department of Engineering, University of Cambridge, CB2 1PZ, UK

Abstract

Geometric stability is a necessary criterion to guarantee stable equilibrium in engineering structures. However, we generally encounter enormous calculations to examine the geometric stability when we make variations on the geometry or the connectivity of a given kinematically and statically indeterminate structure. This study describes how symmetry is utilized to enhance the mobility and geometric stability analysis of symmetric skeletal structures. Symmetry-extended mobility distinguishes representations of the internal mechanisms and self-stress states from relative mobility based on their inherent symmetries using group-theoretic method. Thus, it acts as an efficient tool to evaluate the order of internal mechanisms that may be indistinguishable by traditional structural approaches. Further, it is used to gain effective insights into the mobility and geometric stability of a symmetric skeletal structure with symmetrically perturbed connectivity or geometry. The first-order changes of symmetry-extended mobility are deduced to describe the changes induced by the variations of nodal coordinates, members, and kinematic constraints, respectively. Examples are given to verify the correctness and effectiveness of the proposed method. We show that the geometry or connectivity of kinematically indeterminate symmetric skeletal structures can be altered while at the same time retaining geometric stability and some or all of the original symmetry. The results have potential application in the design of novel deployable structures.

Keywords: Mobility; Kinematically indeterminate; Group theory; Initial imperfection; Kinematic constraint; Removal of members.

*Corresponding author. Tel.: +86 025 83793150; fax: +86 025 83373870.
Email address: fengjian@seu.edu.cn (J. Feng)

1. Introduction

Geometric stability is necessary to guarantee stable equilibriums. It is defined as a property of a structure which preserves its geometry under loads and allows the structure to act as a unified system (Macdonald, 2007). Some questions on this topic such as "what conditions are necessary/sufficient for geometric stability?", "What static or kinematic characteristics of a structure will change or remain constant under varied geometries?" attract great attention and interest among researchers. These questions are crucial for many applications in the fields of civil and mechanical engineering, e.g., for developing novel deployable structures or kinematically indeterminate structures.

Exploring answers to the above questions, Maxwell (1864) developed a mobility rule for pin-jointed structures. More recently, Pellegrino and Calladine (1986) classified these structures into four types according to static and kinematic indeterminacy, and proposed a criterion (Calladine and Pellegrino, 1991) for evaluating their geometric stability. Using constraint equations and a statical-kinematic stiffness matrix, Kuznetsov (1991) studied the kinematic mobility and statical possibility of self-stress states, and proposed a criterion for immobility.

Further, most skeletal structures are symmetric (Guest et al., 2010; Wei and Dai, 2010), as they can be transformed into configurations that are physically indistinguishable from the original configuration. Recently, group theory has been utilized as a systematic mathematical tool for studying the stability of symmetric structures (Kaveh and Nikbakht, 2008; Kettle, 2008; Zingoni, 2009; Kaveh and Nikbakht, 2010), as well as for designing novel deployable structures based on an existing deployable structure (Sareh and Guest, 2015a; Sareh and Guest, 2015b). These group-theoretic methods not only reduce the computational effort, but also give qualitative benefits and insights (Chen et al., 2014; Zingoni, 2014). Based on the irreducible representations of symmetry groups, Guest and Fowler proposed a symmetry-extended mobility rule for symmetric frameworks (Fowler and Guest, 2000; Guest and

Fowler, 2005). Using the symmetry-extended mobility rule, Guest and Fowler (2007) further identified the symmetries of the internal mechanisms and self-stress states, and thus revealed mobility. Therefore, the geometric stability of some symmetric structures with internal mechanisms can be computed efficiently. The recent examples are illustrated in the cyclically symmetric pin-jointed structures (Chen et al., 2013) and the highly symmetric over-constrained structures (Chen et al., 2012). To provide necessary stability conditions, Connelly et al. (2009) and Chen et al. (2014) used group theory to study the stability of symmetric pin-jointed structures. Zhang et al. (2009) used group theory to investigate the geometric configurations and stability of symmetric tensegrity structures. In addition, group theory can be extended to analyze the mobility and geometric stability of finite mechanisms (Zhao et al., 2009; Ding et al., 2011; Wei et al., 2014; Wei and Dai, 2014) that were explored with screw theory.

As geometric stability has often been evaluated by the positive definiteness of the geometric stiffness matrix, Guest (2006) developed stiffness formulations for prestressed pin-jointed structures. Based on the energy method (Connelly, 1982; Connelly and Whiteley, 1996), Vassart et al. (2000) studied the geometric stability of kinematically and statically indeterminate structures. The reported algorithm is capable of identifying the order of internal mechanisms. Using the principle of potential energy, Kovacs and Tarnai (2009) investigated the equilibrium and geometric stability of bar-and-joint assemblies on the surface of a sphere. Masic et al. (2005) studied the geometric stability of symmetric tensegrity structures with shape constraints. It has been proved that the structural equilibrium is preserved under affine node position transformations. Sultan et al. (2001) formulated the general geometric stability conditions for tensegrity structures. The stability conditions were expressed as a set of nonlinear equations and inequalities on the tendon tensions. Subsequently, Sultan (2013) presented the necessary and sufficient conditions for the exponential stability of prestressable pin-jointed structures, and discussed the advantages of the formulation of the tangent stiffness matrix in analytical manipulations and computations. Meanwhile, some studies have evaluated the geometric stability of a pin-jointed structure by heuristic optimization methods

such as genetic algorithms and the ant colony algorithms (El-Lishani et al., 2005; Chen et al., 2012; Koohestani, 2013).

Nevertheless, the above methods usually concern the mobility and geometric stability of a structure with a specific and fixed geometry and connectivity. However, in the preliminary analysis or design process of a structure, the geometry or connectivity might be variable (Zhang et al., 2014). Obviously, repeated calculations for the geometric stability of a structure with variable geometry or connectivity are computationally expensive. Therefore, more efficient numerical methods are required to reduce the relevant computational tasks. Furthermore, it is known that many factors affect the mobility and geometric stability of a structure. Using the singular value decomposition technique, Lu et al. (2007) analyzed the mobility and geometric stability of kinematically indeterminate pin-jointed structures under external loads. They showed that a deployable structure can preserve its geometric stability in certain conditions. Among the components of the stiffness matrices, the main factors affecting the geometric stability of the structure include nodal coordinates, the connectivity patterns of members, and kinematic constraints (Deng and Kwan, 2005; Ohsaki and Zhang, 2006; Chen et al., 2014).

This study explores the impact of symmetric variations on the mobility and geometric stability of symmetric skeletal structures. We proposed a symmetry method that builds on our previous work (Chen et al., 2012; Chen et al., 2014) and the work by Guest and co-workers (Fowler and Guest, 2000; Connelly et al., 2009; Guest et al., 2010). Specifically, we investigate the variations of nodal coordinates, structural members, and kinematic constraints of the structures to provide effective insights into their mobility and geometric stability.

The article is organized as follows. Section 2 introduces the symmetry-extended mobility rule for kinematically indeterminate structures under symmetric variations. Current numerical approaches for evaluating the mobility and geometric stability of a structure are described in Section 2.1. Previous work on the symmetry representations of mechanism modes and self-stress states is presented in Section 2.2. The first-order variations of symmetry-extended mobility for structures with varied connectivity or geometry are derived in Section 2.3. Based

on the proposed method, Section 3 presents the impact of the nodal coordinates on the geometric stability of a structure. In the same section, the effect of symmetry migrations is discussed. Sections 4 and 5 demonstrate the impact of the structural members and the impact of the kinematic constraints on the geometric stability of a structure, respectively. Section 6 concludes the paper.

2. Symmetry-Extended Mobility for Structures under Symmetric Variations

2.1 Mobility of a structure

Maxwell's rule (Maxwell, 1864) is a necessary condition for the mobility of pin-jointed structures by counting structural components. It is valid for kinematically determinate structures; for statically and kinematically indeterminate structures (Pellegrino and Calladine, 1986), Maxwell's rule should be expressed as:

$$m - s = T \cdot j - b - k \tag{1}$$

where T is the magnitude of the rigid-body translation vector, j is the number of all the pin-joints (including boundary nodes), b is the number of members, and k is the number of constraints on the structure (Guest et al., 2010). However, for a free-standing structure (i.e., k=0), k is modified as $k = T + R$ to exclude rigid-body motions, where R is the magnitude of the rigid-body rotation vector (Chen et al., 2014).

In Eq. (1), m is the number of internal mechanism modes, which are the independent vectors in the nullspace of the compatibility matrix $\boldsymbol{J}$, i.e., a solution to the compatibility equation (Pellegrino and Calladine, 1986; Fowler and Guest, 2000):

$$\boldsymbol{Jd} = \boldsymbol{0} \tag{2}$$

where $\boldsymbol{d}$ is a vector of nodal displacements. Moreover, in Eq. (1), s is the number of self-stress states, which are the independent vectors in the nullspace of the equilibrium matrix $\boldsymbol{H}$, i.e., a solution to the equilibrium equation (Pellegrino and Calladine, 1986):

$$\boldsymbol{Ht} = \boldsymbol{0} \tag{3}$$

where $\boldsymbol{t}$ is the vector containing the internal forces in the members. Using the virtual work principle, it can be shown that $\boldsymbol{H} = \boldsymbol{J}^{\mathrm{T}}$.

The relative mobility, $m - s$ in Eq. (1), is not sufficient to evaluate the geometric stability of statically and kinematically indeterminate structures. Calladine and Pellegrino (1991) proposed a criterion to identify whether self-stress states can stiffen all the internal mechanism modes. The criterion is equivalent to the positive definiteness of the quadratic form of the geometric stiffness matrix $\boldsymbol{K}_G$ (Guest, 2006; Ohsaki and Zhang, 2006) satisfying

$$\boldsymbol{\beta}^{\mathrm{T}}\boldsymbol{M}^{\mathrm{T}}\boldsymbol{K}_G\boldsymbol{M}\boldsymbol{\beta} > 0, \qquad \forall \boldsymbol{\beta} \in \Re^m \tag{4}$$

where $\boldsymbol{M}$ is the mechanism mode matrix, and $\boldsymbol{\beta}$ is an arbitrary nonzero vector. Recent work (Deng and Kwan, 2005; Chen et al., 2012; Sultan, 2013) reveals that the criterion provides a necessary condition for the stability of pin-jointed structures. Based on energy theory, a general condition for guaranteeing structural stability can be expressed as:

$$\delta\boldsymbol{d}^{\mathrm{T}}\boldsymbol{K}_T\delta\boldsymbol{d} > 0 \tag{5}$$

where $\boldsymbol{K}_T$ is the tangent stiffness matrix, and $\delta\boldsymbol{d}$ is the virtual nodal displacement vector.

On the other hand, the generalized mobility criterion for over-constrained structures (Guest and Fowler, 2005; Chen et al., 2012) can be written in its modern form as:

$$m - s = (T + R) \cdot (j - b - 1) + \sum_{i=1}^{b} f_i \tag{6}$$

In Eq. (6), j is the number of generalized joints, b is the number of members, and f_i is the dimension of the relative freedoms permitted by member *i*.

2.2 Symmetry-extended mobility rule

The mobility criteria described by Eqs. (1) and (6) express only a relationship between the number of mechanism modes and the number of self-stress states. They are not sufficient to identify the rigidity of a structure. The symmetry method based on group theory can not only detect rigidity/mobility from the results obtained through different symmetry operations (Fowler and Guest, 2000; Guest and Fowler, 2005), but also reveal the geometric stability of

symmetric structures (Guest and Fowler, 2007; Chen et al., 2012). For symmetric pin-jointed structures, the symmetry-extended mobility rule can be written as:

$$\Gamma(m)-\Gamma(s)=\Gamma_T\cdot\Gamma(j)-\Gamma(b)-\Gamma_k \tag{7}$$

where $\Gamma(m)$ is the representation of mechanism modes, $\Gamma(s)$ is the representation of self-stress states, $\Gamma(j)$ is the representation of unshifted joints, and $\Gamma(b)$ is the representation of unshifted members. Γ_T and Γ_k are the representations of rigid-body translations and kinematic freedoms. Furthermore, for symmetric over-constrained structures, the symmetry-extended mobility rule (Guest and Fowler, 2005) has the following form:

$$\Gamma(m)-\Gamma(s)=(\Gamma_T+\Gamma_R)\cdot\left[\Gamma(j)-\Gamma(b)-\Gamma_0\right]+\Gamma_k \tag{8}$$

where Γ_R and Γ_0 are the representations of rigid-body rotations and full symmetry. It should be noted that Γ_T, Γ_R, and Γ_0 can be directly read from the point group theory tables (Altmann and Herzig, 1994). $\Gamma(j)$, $\Gamma(b)$, and Γ_k can be obtained through evaluating the corresponding characters associated with different symmetry operations.

Based on point group theory and its matrix representations, $\Gamma(m)-\Gamma(s)$ can be decomposed into combinations of certain irreducible representations (Guest and Fowler, 2005; Chen et al., 2012):

$$\Gamma(m)-\Gamma(s)=\sum_{i=1}^{\mu}\alpha_i\Gamma_i \tag{9}$$

where α_i is the coefficient for the ith irreducible representation Γ_i of the symmetry group, and μ is the total number of the irreducible representations. As $\Gamma(m)$ and $\Gamma(s)$ must contain non-negative numbers of Γ_i, they are accordingly separated by the sign of α_i. Hereafter, we will demonstrate that the geometric stability of symmetric structures can be revealed relying on the symmetry conditions (Guest and Fowler, 2007).

2.3 Variations of symmetry-extended mobility for structures with varied connectivity or geometry

If the geometry or connectivity of a symmetric structure is variable, the symmetry-extended mobility $\Gamma(m)-\Gamma(s)$ is a function of unshifted joints, members, and kinematic constraints. Hence, $\Gamma(m)-\Gamma(s)$ in Eqs. (7) and (8) can be rewritten in a compact form as:

$$\Gamma(m)-\Gamma(s)=F_G\left(j,b,k\right) \tag{10}$$

where F_G is defined as the general function for obtaining symmetry-extended mobility, and subscript G is the symmetry group of the structure.

Using the original structure as a basic model, the mobility of a structure with varied connectivity or geometry can be given as:

$$\Gamma(m)-\Gamma(s)=F_G^0\left(j,b,k\right)+F_G\left(\Delta j\right)+F_G\left(\Delta b\right)+F_G\left(\Delta k\right) \tag{11}$$

where $F_G^0\left(j,b,k\right)=\Gamma^0(m)-\Gamma^0(s)$ is the mobility of the original structure, and $\Gamma^0(m)$ and $\Gamma^0(s)$ are the representations of the initial mechanism modes and self-stress states, respectively. $F_G\left(\Delta j\right)$, $F_G\left(\Delta b\right)$, and $F_G\left(\Delta k\right)$ are the first-order changes of mobility induced by the variations of joints, members, and kinematic constraints, respectively. It should be noted that the mobility and stability of the original structure ought to be known in advance, which can be obtained using conventional numerical methods (Calladine and Pellegrino, 1991; Guest, 2006). Moreover, the symmetry representations $\Gamma^0(m)$ and $\Gamma^0(s)$ of the original structure should be known in advance, which can be evaluated by group theory and the symmetry-extended mobility rule (Guest and Fowler, 2007; Chen et al., 2014). Consequently, the symmetry-extended expression shown in Eq. (11) provides effective insights into the evaluation of the mobility and geometric stability of symmetric structures with varied connectivity or geometry. In this equation, only the representations of $F_G\left(\Delta j\right)$, $F_G\left(\Delta b\right)$, and $F_G\left(\Delta k\right)$ need to be identified. Thus, in comparisons with conventional approaches, this symmetry method not only on the one hand avoids repeated derivations and calculations for the associated matrices, such as the equilibrium matrix and the tangent stiffness matrix, but also on the other hand provides an efficient method for identifying whether a structure becomes unstable after making geometric variations.

It is important to point out that, in some cases, geometric variations may break some symmetry operations of the original structure. In these cases, the symmetry group G of the structure will descend into a subgroup $G_1 \subset G$ (Altmann and Herzig, 1994). Accordingly, the symmetry-extended mobility is rewritten based on subgroup G_1 as:

$$\Gamma(m)-\Gamma(s)=F_{G_1}^{0}(j,b,k)+F_{G_1}(\Delta j)+F_{G_1}(\Delta b)+F_{G_1}(\Delta k) \tag{12}$$

3. Impact of the Nodal Coordinates on Geometric Stability

Nodal coordinates are the basic factors which determine the geometric configuration of a structure (Zhang et al., 2009). For kinematically indeterminate structures, any changes of nodal coordinates are likely to influence their geometric stability. Making variations on a symmetric structure while preserving its connectivity and kinematic constraints, the structure either retains its original symmetry, or transforms into a structure with a low-order symmetry.

3.1 Invariant initial symmetry

A symmetric structure can retain its initial symmetry group, if its nodal coordinates are modified by rigid-body motions, linear scaling, or symmetry operations. According to Ohsaki and Zhang's investigation (Ohsaki and Zhang, 2006), rigid-body motions and linear scaling do not affect the structural stability. Under any symmetry operation *S*, the geometric stability of a structure remains unchanged and this can be proved and illustrated as follows.

Considering the case that a structure is under a symmetry operation *S* (e.g., rotation and reflection), the nodal displacements $\boldsymbol{d}$ and external loads $\boldsymbol{P}$ on the structure in the new configuration will then be:

$$\boldsymbol{d}_S=\boldsymbol{R}_S\cdot\boldsymbol{d}\ ,\ \boldsymbol{P}_S=\boldsymbol{R}_S\cdot\boldsymbol{P} \tag{13}$$

where $\boldsymbol{R}_S$ is the nodal transformation matrix under the symmetry operation *S*, and $\boldsymbol{d}_S$ and $\boldsymbol{P}_S$ are the corresponding displacement and load vectors, respectively.

Further, the deformation vector $\boldsymbol{e}$ of the members is:

$$\boldsymbol{e}_s = \boldsymbol{T}_S \cdot \boldsymbol{e} \tag{14}$$

where $\boldsymbol{T}_S$ is the member transformation matrix under the symmetry operation S, and $\boldsymbol{e}_s$ is the deformation vector in the new configuration. The equilibrium equation and the compatibility equation of the structure, respectively, are given by:

$$\boldsymbol{K}_{T,S}\boldsymbol{d}_S = \boldsymbol{K}_{T,S}\boldsymbol{R}_S \cdot \boldsymbol{d} = \boldsymbol{P}_S \tag{15}$$

$$\boldsymbol{J}_S\boldsymbol{d}_S = \boldsymbol{J}_S\boldsymbol{R}_S \cdot \boldsymbol{d} = \boldsymbol{e}_S \tag{16}$$

where $\boldsymbol{K}_{T,S}$ is the symmetry-adapted tangent stiffness matrix, and $\boldsymbol{J}_S$ is the symmetry-adapted compatibility matrix. Substituting Eqs. (13) and (14) into Eqs. (15) and (16), the matrices $\boldsymbol{K}_{T,S}$ and $\boldsymbol{J}_S$ have the form:

$$\boldsymbol{K}_{T,S} = \boldsymbol{R}_S^{\mathrm{T}}\boldsymbol{K}_T\boldsymbol{R}_S,\ \boldsymbol{J}_S = \boldsymbol{T}_S^{\mathrm{T}}\boldsymbol{J}\boldsymbol{R}_S \tag{17}$$

It is known that the eigenvalues of a matrix remain invariant under similarity transformations (Chen and Feng, 2012). Hence, both $\boldsymbol{K}_{T,S}$ and $\boldsymbol{J}_S$ in Eq. (17) preserve their original eigenvalues. In other words, the mobility and geometric stability of a structure remain unchanged under symmetry operations.

Moreover, the symmetry of a structure remains invariant even though some nodes are displaced from their initial locations. As a result, it cannot be intuitively identified whether the minimum eigenvalue of $\boldsymbol{K}_T$ or $\boldsymbol{J}$ associated with the new configuration changes. Actually, the mobility and geometric stability can be detected from the symmetries of the mechanism modes and self-stress states according to Eq. (11). Since both the number of unshifted nodes and members and the group G do not change, the symmetry-extended mobility is independent of the changes of nodal coordinates. That is $F_G(\Delta j) = F_G(\Delta b) = F_G(\Delta k) = 0$, which leads to

$$\Gamma(m) - \Gamma(s) = F_G^0(j, b, k) + 0 = \Gamma^0(m) - \Gamma^0(s) \tag{18}$$

Therefore, the mechanism modes and the self-stress states preserve the original symmetries, and the geometric stability of the structure remains unchanged.

This can be illustrated with examples on three-dimensional C_{2nv} symmetric pin-jointed structures as follows. These pin-jointed structures consist of $2n$ bottom nodes, $2n$ top nodes,

and $6n$ bars. The bottom nodes are constrained in three directions. The radius of the circles formed by the top and bottom nodes are r_s and r_d, respectively, and the height is h. For the original structures, it satisfies $r_s = r_d = h$. Such structures remain unchanged under the identity operation E, $2n-1$ rotation operations C_{2n}^i ($i \in [1, 2n-1]$) around the Z axis, and $2n$ mirror operations σ_i ($i \in [1, 2n]$). For instance, Fig. 1 shows the symmetry operations of one type of the C_{2nv} symmetric structures, i.e., a C_{4v} symmetric structure.

These symmetric structures have one mechanism mode (i.e. m=1) and one self-stress state (i.e. s=1). The mechanisms cannot be stiffened and are finite mechanisms (Tarnai, 1980; Sultan, 2013). Thus, the structures retain full symmetry in the group C_{nv} (Guest and Fowler, 2007; Chen et al., 2014). Affected by the variations of the nodal coordinates, r_s, r_d, and h are no longer equal; however, the structure still belongs to the group C_{2nv}. Both $\Gamma(j)$ and $\Gamma(b)$ remain invariant under symmetry operations. Table 1 gives the calculations of the relative degrees of freedom.

The relative degrees of freedom in the symmetry group C_{2nv} can be further reduced to:

$$\Gamma(m) - \Gamma(s) = B_1 - B_2 \tag{19}$$

Then, symmetry representations of the mechanism mode and self-stress state are:

$$\Gamma(m) = B_1, \ \Gamma(s) = B_2 \tag{20}$$

The mechanism $\Gamma(m) = B_1$ is not fully symmetric. At this point, it is difficult to distinguish whether the mechanism is finite. Supposing that the structure is perturbed by a tiny deformation with B_1 symmetry; the symmetry of the geometric configuration migrates from group C_{2nv} to C_{nv}. $\Gamma(m) - \Gamma(s)$ is further evaluated in the subgroup C_{nv}:

Group C_{nv}	E	$C_{2n}^i, i \in [1, 2n-1]$	$\sigma_i, i \in [1, n]$
$\Gamma(m) - \Gamma(s)$	0	0	2

(21)

This can be expressed in terms of the irreducible representations as:

$$\Gamma(m) - \Gamma(s) = A_1 - A_2 \tag{22}$$

Therefore, the symmetry representations of the mechanism mode and self-stress state are:

$$\Gamma(m) = A_1,\ \Gamma(s) = A_2 \tag{23}$$

Eq. (23) shows that the low-order symmetric self-stress state cannot stiffen the fully symmetric mechanism mode. Hence, the C_{2nv} symmetric structures with new configurations remain unstable. Although subjected to the changes of nodal coordinates, they are finite mechanisms. Meanwhile, the kinematic characteristics remain unchanged, where the internal mechanism retains A_1 symmetry and the self-stress state retains A_2 symmetry in the group C_{nv}.

In order to verify the static and kinematic characteristics of the structures, in this section, the force method and the singular value decomposition are employed and adapted such that computer program is constructed leading to the intuitive illustration of the results. The parameters r_s and h are varied, whereas r_d and the symmetry groups of the structures are kept unchanged. Figure 2 shows the minimum and second-smallest singular values of $\boldsymbol{J}$ for the C_{4v} symmetric structures with different r_s and h. Figure 3 shows those values for the C_{16v} symmetric structures.

It can be shown that, by making variations on r_s and h, the singular values change accordingly. Nevertheless, all the minimum singular values can be assumed to be zero, as they are smaller than 10^{-12}. The second-smallest singular values are nonzero, whereas the minimum is greater than 10^{-3}. Hence, these symmetric structures with varied nodal coordinates have a single mechanism mode and self-stress state.

In addition, the impact of nodal coordinates induced by different r_s and r_d is investigated, where the height h and the symmetry groups of the structures remain unchanged. The corresponding results of singular values of $\boldsymbol{J}$ for the C_{4v} symmetric and C_{20v} symmetric structures are shown in Fig. 4 and Fig. 5, respectively.

It can be seen from Figs. 4 and 5 that the singular values change significantly with the variations of r_s and r_d. The minimum singular values continue to be zero, while the second-smallest singular values are nonzero. It means that the compatibility matrix $\boldsymbol{J}$ has necessarily a zero singular value, regardless of the variations of r_s and r_d. As a result, the symmetric

structures have a single mechanism mode and self-stress state. It should be noted that the results are consistent with those obtained from the symmetry analysis (see Eq. (23)). Therefore, variations of nodal coordinates do not alter the mobility or geometric stability of a symmetric structure as long as the original symmetry is retained.

3.2 Migration to a lower-order symmetry group

Admittedly, geometric position deviations of joints exist in engineering structures, caused by initial imperfections and uncertain errors. It tends to break the perfect symmetry of a structure. If the geometric locations of nodes are close to the ideal ones, small position deviations do not destruct the total symmetric properties of the structure. However, in this case, the initial symmetry group G migrates to a lower-order symmetry group $G_1 \subset G$, whereas the structure maintains partial symmetry properties in the initial symmetry group G. And in such a case, mobility and geometric stability of a structure can be subsequently re-evaluated in the subgroup G_1 (see Eq. (12)).

A C_{6v} symmetric pin-jointed structure is given as an example so as to illustrate and verify the above statement. For the C_{6v} symmetric structure, the original geometric configuration is in accordance with the C_{2nv} symmetric structures shown in Fig. 1. The geometric parameters are taken as $r_s = 0.8$, $r_d = h = 1$. Recall that the initial structure with perfect symmetry is mobile, and has $m = 1$ mode of internal mechanism and $s = 1$ state of self-stress. The internal mechanism and self-stress state are expressed in symmetry representations as $\Gamma(m) = B_1$, and $\Gamma(s) = B_2$. Table 2 shows the static and kinematic characteristics of the initial C_{6v} symmetric structure. It also presents the symmetry reduction of the structure because of different position deviations. The first row in the table lists all subgroups of the symmetry group C_{6v} (Altmann and Herzig, 1994): C_{3v}, C_{2v}, C_v, C_6, C_3, C_2, and C_1. Groups such as C_6, C_3, and C_2 do not possess mirror symmetry operations, and the group C_1 has only an identity symmetry operation.

When the geometric position deviations preserve full symmetry (i.e., C_{6v}), the static and kinematic characteristics of the structure remain invariant, and the structure continues to be transformable. Otherwise, the geometric configuration resulted by deviations will have a lower-order symmetry. Figure 6 shows the case that the structure belongs to the symmetry groups C_{3v}, C_{2v} or C_v, where Δ indicates the tiny position deviations of the specified joints. In these cases, as shown in Table 2, symmetries of the mechanisms are higher than those of the self-stress states. The structure cannot maintain a stable equilibrium state. In other words, the structure is a finite mechanism. It should be pointed out that the results obtained in this paper for these three symmetric structures are consistent with those of Kangwai and Guest (1999).

If a symmetric structure has no mirror symmetry operations after geometric deviations, the self-stress state and the mechanism will be equisymmetric (see Table 2). Then the self-stress state can provide first-order stiffness to stiffen the internal mechanism. Therefore, geometric stability and kinematic characteristics of the structure can be different from those of the original structure.

A C_{8v} symmetric structure is presented in Fig. 7, where $r_s = 0.8$, and $r_d = h = 1$. First-order analysis reveals that the structure has $m = 1$ mechanism mode and $s = 1$ self-stress state. The symmetry representation of the mechanism mode is $\Gamma(m) = B_1$, and that of the self-stress state is $\Gamma(s) = B_2$. It turns out that the structure is unstable. To study the impact of position deviations to different symmetries, Table 3 shows the static and kinematic characteristics of the C_{8v} symmetric structure with reduced symmetries. In the table, symmetry groups C_{4v}, C_{2v}, C_v, C_8, C_4, C_2 and C_1 are subgroups of the group C_{8v}.

Figure 7 shows the case in which the geometric configuration belongs to the symmetry groups C_{4v}, C_{2v} or C_v. It can be noticed from Table 3 that, while the mechanism mode of the structure is fully symmetric, the self-stress state is symmetric with a lower-order. Therefore, the internal mechanism cannot be stiffened, and the structure is still unstable.

Nevertheless, if the structure has no mirror symmetry operations and migrates to C_8, C_4,

C_2 or C_1 symmetric after geometric deviations, the self-stress state and the mechanism will be equisymmetric, as listed in Table 3. In this case, it is difficult to identify whether the mechanism mode is infinitesimal. Geometric stability and kinematic characteristics of the structure should be evaluated using the energy method.

4. Impact of the Structural Members on Geometric Stability

A structure is composed of a number of joints and members according to specific geometric topology. Each type of members plays a unique role in maintaining the structural stability. In engineering design, the determination of key members plays an important role in evaluating structural safety and reliability (Murtha-Smith, 1988; Sebastian, 2004; Deng and Kwan, 2005). For a structure with *s* modes of static indeterminacy, the removal of a member is not arbitrary. Sometimes, in a statically determinate structure, the removal of a single member might result in geometric instability. In such cases, the member is identified as a necessary (non-removable) member of the structure. In structural analysis, it is important to identify efficiently whether the removal of multiple members leads to structural instability.

To identify necessary members for a statically indeterminate structure, a conventional method is re-evaluating the singular values of the compatibility matrix and the eigenvalues of the stiffness matrices. In fact, since engineering structures have numerous joints and members, various geometric configurations can be obtained after removing some members in certain ways. Consequently, extracting the singular values of the compatibility matrix and evaluating the positive definiteness of stiffness matrices for each possible configuration is computationally expensive. Here, symmetry is adopted for a systematic classification and removal of the members of structures. The symmetry method can efficiently distinguish the static and kinematic characteristics of a structure after the removal of a single or multiple members, resulting in revealing its structural stability.

4.1 Representation of the changed members

According to Eq. (7), the symmetry-extended mobility of the original structure can be expressed as:

$$\Gamma^0(m)-\Gamma^0(s)=\Gamma_T\cdot\Gamma^0(j)-\Gamma^0(b)-\Gamma_k^0 \tag{24}$$

where $\Gamma^0(m)$ and $\Gamma^0(s)$ are the representations of the mechanisms and self-stress states of the original structure. $\Gamma^0(j)$ and $\Gamma^0(b)$ are the representations of unshifted nodes and members. Γ_k^0 is the representation of invariant kinematic constraints. If the structure has no constraints, then $\Gamma_k^0=\Gamma_T+\Gamma_R$. Γ_T and Γ_R are the representations of rigid-body translations and rotations.

The geometry of a structure changes if a number of members are removed from the original configuration. Let t denote the way of removing the members, we can rewrite the symmetry-extended mobility of the new structure as:

$$\Gamma^{\mathrm{t}}(m)-\Gamma^{\mathrm{t}}(s)=\Gamma_T\cdot\Gamma^{\mathrm{t}}(j)-\Gamma^{\mathrm{t}}(b)-\Gamma_k^{\mathrm{t}} \tag{25}$$

where $\Gamma^{\mathrm{t}}(m)$ and $\Gamma^{\mathrm{t}}(s)$ are the representations of the mechanisms and self-stress states under the action of t. $\Gamma^{\mathrm{t}}(j)$ and $\Gamma^{\mathrm{t}}(b)$ are the new representations of unshifted nodes and members. Γ_k^{t} is the new representation of invariant kinematic constraints. The unshifted nodes and kinematic constraints remain the same after the removal of the members, i.e., $\Gamma^{\mathrm{t}}(j)=\Gamma^0(j)$ and $\Gamma_k^{\mathrm{t}}=\Gamma_k^0$. Subtracting Eq. (24) from Eq. (25), we obtain the representation of the changed members:

$$F_G(\Delta b)=\Delta\Gamma(m)-\Delta\Gamma(s)=\Delta\Gamma(b) \tag{26}$$

where $\Delta\Gamma(m)=\Gamma^{\mathrm{t}}(m)-\Gamma^0(m)$ and $\Delta\Gamma(s)=\Gamma^{\mathrm{t}}(s)-\Gamma^0(s)$ are the representations for the changes of the mechanism modes and self-stress states after removing some members. $\Delta\Gamma(b)=\Gamma^0(b)-\Gamma^{\mathrm{t}}(b)$ describes the change of the representation of the unshifted members, which can reveal the symmetry of the removed members.

We note that the symmetry representations $\Gamma^0(m)$, $\Gamma^0(s)$ and $\Gamma^0(b)$ of the original structure are known in advance. Then, according to Eqs. (11) and (26), the symmetry of the new mechanism modes and self-stress states can be obtained, combined with the change of

the representation induced by varied connectivity. Subsequently, the static and kinematic characteristics of the new structure can be evaluated. Hence, there is no need for repeated calculations on the compatibility matrix and stiffness matrices. The method takes advantage of the symmetry of the changed members, and significantly improves the computational efficiency.

4.2 2D symmetric frameworks with selected members removed

Figure 8(a) illustrates a 2D symmetric structure, which consists of 6 pin-joints and 15 members. Members 1~6 are the boundary elements, members 8, 11 and 13 are the main diagonal elements, and the others are the secondary diagonal elements.

The initial structure remains invariant under the following operations: the identity operation *E*, five rotational operations about the Z-axis $C_6^1 \sim C_6^5$, and six mirror operations $\sigma_1 \sim \sigma_6$. Therefore, the structure has 12 independent symmetry operations, and belongs to the symmetry group C_{6v}.

The rank of the compatibility matrix $\boldsymbol{J}$ turns out to be $r = 9$ by extracting the singular values. Thus, the structure is kinematically determinate and statically indeterminate, as it has $s = 6$ independent self-stress states. Accordingly, the maximum number of members that can be removed from the structure is six. To obtain the mobility, $\Gamma(m) - \Gamma(s)$ is evaluated in the group C_{6v}:

Group C_{6v}	E	$2C_6$	$2C_3$	C_2	$3\sigma_v$	$3\sigma_d$
$\Gamma(m) - \Gamma(s)$	–6	–2	0	–2	–2	–2

(27)

where $\Gamma(m) - \Gamma(s)$ is reduced as:

$$\Gamma(m) - \Gamma(s) = -2A_1 - E_1 - E_2 \tag{28}$$

As $m = 0$ and $s = 6$, the representations of the mechanism and self-stress states are:

$$\Gamma(m) = \varnothing,\ \Gamma(s) = 2A_1 + E_1 + E_2 \tag{29}$$

The structure has $s = 6$ self-stress states with different symmetry properties, which contain the full symmetry A_1. To identify the necessary members, the mobility of the resulting structures with a single member removed from the original structure is studied. Three distinct configurations exist after removing a single member from the structure, shown in Fig. 8(b-d). Based on the irreducible representations of the symmetry groups, the results of structures with different member removed are studied and listed in Table 4.

According to the symmetry of the removed bar $\Delta\Gamma(b)$, the symmetry of the structure changes from the group C_{6v} to the groups C_{2v} or C_v after removing a single member, but the mechanism remains invariant. Moreover, the representations of the mechanism and self-stress states are summarized as $\Gamma(m) = \varnothing$ and $\Gamma(s) \neq \varnothing$, respectively. The resulting structures are kinematically determinate and statically indeterminate. In other words, the structure remains stable after removing any one of the members. Hence, the symmetric structure has no necessary members.

Although the 2D structure has only six joints, it has many possible geometric configurations. However, generally, engineering structures have so many joints that optimizing their geometries is complex. Using the inherent symmetry and preserving symmetry operations as many as possible, some independent configurations can be obtained by removing different types of members. For example, the original structure belongs to the group C_{6v}. New C_{6v} symmetric structures can be obtained by removing six interior members or six exterior members, as shown in Fig. 9(a) and Fig. 9(b), respectively. The symmetries of these structures are equivalent. Similarly, if some members of low-order symmetry are removed, the corresponding structure will fall into the subgroups C_{3v}, C_{2v}, C_3 or C_v, as shown in Fig. 9(c-h). Then, the mobility and geometric stability of the structure is re-identified within the relevant subgroup, listed in Table 5.

The results of the proposed method are consistent with those from the first-order analysis, as listed in the last column of Table 5. In addition, removing the fully symmetric members necessarily causes the decrease of the combinatorial coefficient of A_1, which is a

representation of the self-stress states. Accordingly, it tends to change the static and kinematic indeterminacy of the structure. If the representations of the removed members contain more than one kind of irreducible representation, the mobility and kinematic indeterminacy of the structure would be sensitive to the removal of members. Then the structure would generate new internal mechanisms, such as the structures in Fig. 9(e) or Fig. 9(f).

4.3 Mobility of symmetric Kiewitt type structures with certain members removed

Figure 10 shows a symmetric Kiewitt type structure (Fan et al., 2012), where the numbers of pin-joints and members are $j=56$ and $b=145$, respectively. The outmost 18 boundary joints are constrained in three directions.

As shown in Fig. 10, the geometric configuration of the structure remains invariant under the following operations: the identity operation E, five rotation operations $C_6^1 \sim C_6^5$ about the Z-axis, and six mirror operations $\sigma_1 \sim \sigma_6$ along the Z-axis. The structure has twelve independent symmetry operations and thus belongs to the group C_{6v}. Using the singular value decomposition, the rank of the equilibrium matrix $\boldsymbol{H}$ of the structure turns out to be $r=114$. The symmetric structure has no internal mechanism, however, has $s=31$ independent self-stress states. Thus, the structure is an over-constrained stable structure, and at most thirty-one members can be removed. To identify the necessary members, the symmetry-extended mobility $\Gamma(m)-\Gamma(s)$ is evaluated in the group C_{6v}, given as:

Group C_{6v}	E	$2C_6$	$2C_3$	C_2	$3\sigma_v$	$3\sigma_d$
$\Gamma(m)-\Gamma(s)$	-31	3	-1	-3	-7	1

(30)

In Eq. (30), $\Gamma(m)-\Gamma(s)$ can be expressed as:

$$\Gamma(m)-\Gamma(s)=-4A_1-A_2-5B_1-B_2-4E_1-6E_2 \tag{31}$$

As $m=0$ and $s=31$, the representations of the mechanism and self-stress states are:

$$\Gamma(m)=\varnothing,\ \Gamma(s)=4A_1+A_2+5B_1+B_2+4E_1+6E_2 \tag{32}$$

$\Gamma(s)$ in Eq. (32) contains the item A_1, indicating that some of the self-stress states are fully symmetric. Figure 11 shows eleven independent configurations of the symmetric structure with the removal of a single member. In the figure, "☆" is used to depict the removed member.

The mobility and geometric stability of the obtained configurations are evaluated. Table 6 gives the symmetry results. It can be seen from Table 6 that the symmetry of the structure descends from the group C_{6v} to the groups C_{2v} or C_v, while, that the kinematic and static characteristics remain unchanged. This is because all the representations of the mechanisms are $\Gamma(m)=\varnothing$, and those of the self-stress states are summarized as $\Gamma(s)\neq\varnothing$. The structure remains kinematically determinate and statically indeterminate. Since the structure remains stable with an arbitrary one of the members removed, it possesses no necessary members.

Furthermore, we study the structures with fully symmetric members removed. The eight geometric configurations are shown in Fig. 12, where the symbol "☆" is used to mark the removed members. The symmetry results of the static and kinematic characteristics are listed in Table 7.

The study proved that the static and kinematic characteristics vary only if the inner ring and outer ring circumferential members are removed at the same time (see Fig. 12(h)). The structure has a new internal mechanism after the removal, but maintains its stability. The new mechanism mode is first-order infinitesimal, since it obtains structural stiffness via the self-stress states. On the other hand, removing the vertical members does not affect the rigidity of the original structure. Even if all the vertical members are removed, the structure preserves its geometric stability.

During the analysis process, there is no need to solve the minimum eigenvalues of a series of stiffness matrices or calculating the singular values of the corresponding equilibrium matrices. Therefore, computational tasks are reduced significantly.

5. Impact of the Kinematic Constraints on Geometric Stability

The kinematic constraints (e.g., boundary conditions) are sensitive to the mobility and stability of a structure (Lu et al., 2007; Chen et al., 2013). When the kinematic constraints change, in general, the global equilibrium matrix and the stiffness matrices need to be rebuilt. In this section, using symmetry, the mobility and geometric stability of a structure are evaluated from the variations of symmetries of the internal mechanisms and self-stress states. According to Eqs. (11), (24) and (25), the number of unshifted joints and members remains invariant after changing the kinematic constraints, i.e., $\Gamma^{t}(j)=\Gamma^{0}(j)$ and $\Gamma^{t}(b)=\Gamma^{0}(b)$. Subtracting Eq. (24) from Eq. (25), we obtain the first-order change of the symmetry-extended mobility induced by the kinematic constraints:

$$F_G\left(\Delta k\right)=\Delta\Gamma(m)-\Delta\Gamma(s)=\Delta\Gamma_k \tag{33}$$

where $\Delta\Gamma_k=\Gamma_k^0-\Gamma_k^{t}$ is the representation of the changed kinematic constraints. Eq. (33) also suits a more general over-constrained system (see Eq. (8)).

Eq. (33) can be expressed by certain irreducible representations. Using the symmetry-extended method, the symmetry representations $\Gamma^0(m)$, $\Gamma^0(s)$ and Γ_k^0 of the original structure has been obtained in advance. Therefore, the symmetry of the internal mechanisms and self-stress states of the structures with varied geometric configurations can be efficiently calculated.

5.1 Released degrees of freedom for symmetric structures

Figure 13(a) shows a C_{2v} symmetric over-constrained framework. The simple 2D structure consists of four joints and four link members, where the joints 1 and 3 are pin-joints. The in-plane rotational degrees of freedom of joints 2 and 4 are constrained.

Table 8 shows the relative mobility of the structure under different symmetry operations. On the basis of irreducible representations of the group C_{2v}, the results of $\Gamma(m)-\Gamma(s)$ is reduced into:

$$\Gamma(m)-\Gamma(s)=-B_2 \tag{34}$$

The four-link over-constrained system has no internal mechanism, i.e., $m=0$. Therefore, the symmetries of the internal mechanism and self-stress state are:

$$\Gamma(m)=\varnothing,\ \Gamma(s)=B_2 \tag{35}$$

Figure 13(a) also shows the structure with released rotational degrees of freedom of joints 2 and 4. The variations of the kinematic constraints are listed in the last column of Table 8. They are reduced into:

$$F_G(\Delta k)=\Delta\Gamma_k=A_1+B_2 \tag{36}$$

It is concluded from Eqs. (35) and (36) that, with two degrees of freedom released, the symmetries of the internal mechanism and self-stress state are:

$$\Gamma(m)=A_1,\ \Gamma(s)=\varnothing \tag{37}$$

Hence, the structure transforms from stable into mobile. In fact, as shown in Fig. 13(a), the new structure is a classic four-bar mechanism. Therefore, the results in Eq. (36) and (37) are verified.

In addition, the effect of the kinematic constraints of a C_{3v} symmetric structure on its geometric stability is investigated, as shown in Fig. 13(b-c). The structure is composed of ten pin-joints and 21 bars, whereas the joints 1~4 are totally constrained. Detailed geometric information for the structure is available in the literature (Chen et al., 2013). The relative mobility of the structure under the symmetry operations of E, C_3^1, C_3^2, σ_1, σ_2 and σ_3 are calculated in Table 9.

Based on the irreducible representations of the group C_{3v}, the column of $\Gamma(m)-\Gamma(s)$ in Table 9 is simplified as:

$$\Gamma(m)-\Gamma(s)=-A_1-E \tag{38}$$

Since the structure has no internal mechanism (i.e., $m=0$), the symmetries of the internal mechanism and self-stress states are:

$$\Gamma(m)=\varnothing,\ \Gamma(s)=A_1+E \tag{39}$$

To change the kinematic constraints, the degree of freedom along the *Z* direction of joint 1 is released, as well as the translational degrees of freedom along the mirror planes of joints

2~4. The last column of Table 9 presents the corresponding variations of the kinematic constraints. The results are simplified as:

$$F_G(\Delta k) = \Delta\Gamma_k = 2A_1 + E \tag{40}$$

Combining with Eqs. (39) and (40), the static and kinematic characteristics of the C_{3v} symmetric structure with varied kinematic constraints are:

$$\Gamma(m) = A_1,\ \Gamma(s) = \varnothing \tag{41}$$

Therefore, the structure must be mobile and its static and kinematic indeterminacy change significantly. These results match well with the FEM results in Chen et al. (2013), thus the proposed method is feasible.

5.2 Constrained degrees of freedom for a highly symmetric structure

As shown in Fig. 14(a), the highly symmetric structure is originated from a cube, and consists of eight pin-joints and twelve bars. Typical symmetry operations for the structure are also shown in Fig. 14(a), such as the rotations C_2, C_3, C_4, and the inversion i. Table 10 lists the results of the evaluation of relative mobility under 48 independent symmetry operations.

Based on the irreducible representations of the group O_h, the results of $\Gamma(m)-\Gamma(s)$ in the fifth row of Table 10 are simplified as:

$$\Gamma(m)-\Gamma(s) = T_{2g} + A_{2u} + E_u \tag{42}$$

Since the highly symmetric structure has no redundant constraints, the number of self-stress states is $s = 0$. Therefore, symmetries of the mechanisms and self-stress states are:

$$\Gamma(m) = T_{2g} + A_{2u} + E_u,\ \Gamma(s) = \varnothing \tag{43}$$

The structure has $m = 6$ independent internal mechanisms, associated with multiple low-order symmetry subspaces. To reduce its mobility, the pin-joints and bars are replaced by revolute joints and rigid links, respectively. Figure 14(b) shows the corresponding over-constrained system. Note that, for the link elements, the rotational degrees of freedom around the secondary axis and translational degrees of freedom along the inversion point are

permissible. Consequently, the specific values of $\Delta\Gamma_k$ under different symmetry operations are calculated, and listed in the last column in Table 10. They are simplified as:

$$F_G(\Delta k) = \Delta\Gamma_k = T_{1g} + T_{2g} + A_{1u} + E_u + T_{2u} \tag{44}$$

Combining with Eq. (43) and Eq. (44), the static and kinematic characteristics of the highly symmetric over-constrained system shown in Fig. 14(b) are:

$$\Gamma(m) = A_{2u},\ \Gamma(s) = A_{1u} + T_{1g} + T_{1u} \tag{45}$$

The internal mechanism retains full symmetry in the tetrahedral symmetry subgroup (i.e., $T_d \subset O_h$), but the self-stress states have low-order symmetries. None of the self-stress states can provide first-order stiffness to stiffen the fully symmetric mechanism. Thus, the symmetric over-constrained system is a deployable structure with a single degree of freedom. The conclusion is in agreement with the results in the work of Chen et al. (2012).

6. Conclusions

Many factors affect the mobility and geometric stability of a structure, such as the nodal coordinates of joints, the connectivity of members, and kinematic constraints. This study has introduced symmetry-extended mobility rule and irreducible representations to investigate the geometric stability of a skeletal structure influenced by these factors. Examples on symmetric structures with varied nodal coordinates, structural members, and kinematic constraints have been presented and illustrated. It turns out that a symmetric skeletal structure with kinematic indeterminacy can retain its geometric stability and some or all of the original symmetry, while its geometry or connectivity is altered. The results verify that the symmetry method presented in this paper offers an intuitive and efficient method for characterizing the geometric stability of symmetric skeletal structures. Thus, the proposed method provides a theoretical basis for determining the mobility of structures, designing novel deployable structures, and finding novel statically or kinematically indeterminate systems.

Acknowledgments

This work has been supported by the National Natural Science Foundation of China (Grant No. 51278116), and Scientific Research Foundation of the Graduate School of Southeast University (Grant No. YBPY1201). The first author of this paper would like to acknowledge the China Scholarship Council for supporting his stay at the University of Cambridge and Dr. Simon D. Guest for his guidance and help. Special thanks go to Dr. Guowu Wei from School of Computing, Science & Engineering at the University of Salford for his suggestions. Valuable comments from the anonymous reviewers are also gratefully acknowledged.

References

Altmann, S. L., and Herzig, P., 1994. Point-Group Theory Tables. Clarendon Press, Oxford, UK.

Calladine, C. R., and Pellegrino, S., 1991. First-order infinitesimal mechanisms. International Journal of Solids and Structures 27(4), 505-515.

Chen, Y., Feng, J., and Fan, L., 2013. Mobility and kinematic simulations of cyclically symmetric deployable truss structures. Proceedings of the Institution of Mechanical Engineers, Part C: Journal of Mechanical Engineering Science 227(10), 2218-2227.

Chen, Y., Feng, J., and Wu, Y., 2012. Novel form-finding of tensegrity structures using ant colony systems. Journal of Mechanisms and Robotics 4(3), 31001.

Chen, Y., Feng, J., and Zhang, Y., 2014. A necessary condition for stability of kinematically indeterminate pin-jointed structures with symmetry. Mechanics Research Communications 60, 64-73.

Chen, Y., Guest, S. D., Fowler, P. W., and Feng, J., 2012. Two-orbit switch-pitch structures. Journal of the International Association for Shell and Spatial Structures 53(3), 157-162.

Chen, Y., and Feng, J., 2012. Generalized eigenvalue analysis of symmetric prestressed structures using group theory. Journal of Computing in Civil Engineering 26(4), 488-497.

Connelly, R., 1982. Rigidity and energy. Inventiones Mathematicae 66(1), 11-33.

Connelly, R., Fowler, P. W., Guest, S. D., Schulze, B., and Whiteley, W. J., 2009. When is a

symmetric pin-jointed framework isostatic? International Journal of Solids and Structures 46(3), 762-773.

Connelly, R., and Whiteley, W., 1996. Second-order rigidity and prestress stability for tensegrity frameworks. SIAM Journal on Discrete Mathematics 9(3), 453-491.

Deng, H., and Kwan, A. S. K., 2005. Unified classification of stability of pin-jointed bar assemblies. International Journal of Solids and Structures 42(15), 4393-4413.

Ding, X. L., Yang, Y., and Dai, J. S., 2011. Topology and kinematic analysis of color-changing ball. Mechanism and Machine Theory 46(1), 67-81.

El-Lishani, S., Nooshin, H., N., Disney, and P., D., 2005. Investigating the statical stability of pin-jointed structures using genetic algorithm. International Journal of Space Structures 20(1), 53-68.

Fan, F., Yan, J., and Cao, Z., 2012. Elasto-plastic stability of single-layer reticulated domes with initial curvature of members. Thin-Walled Structures 60(0), 239-246.

Fowler, P. W., and Guest, S. D., 2000. A symmetry extension of Maxwell's rule for rigidity of frames. International Journal of Solids and Structures 37(12), 1793-1804.

Guest, S. D., 2006. The stiffness of prestressed frameworks: A unifying approach. International Journal of Solids and Structures 43(3-4), 842-854.

Guest, S. D., Schulze, B., and Whiteley, W. J., 2010. When is a symmetric body-bar structure isostatic? International Journal of Solids and Structures 47(20), 2745-2754.

Guest, S. D., and Fowler, P. W., 2005. A symmetry-extended mobility rule. Mechanism and Machine Theory 40(9), 1002-1014.

Guest, S. D., and Fowler, P. W., 2007. Symmetry conditions and finite mechanisms. Journal of Mechanics of Materials and Structures 2(2), 293-301.

Kangwai, R. D., and Guest, S. D., 1999. Detection of finite mechanisms in symmetric structures. International Journal of Solids and Structures 36(36), 5507-5527.

Kaveh, A., and Nikbakht, M., 2008. Stability analysis of hyper symmetric skeletal structures using group theory. Acta Mechanica 200(3-4), 177-197.

Kaveh, A., and Nikbakht, M., 2010. Improved group-theoretical method for eigenvalue

problems of special symmetric structures, using graph theory. Advances in Engineering Software 41(1), 22-31.

Kettle, S. F., 2008. Symmetry and Structure: Readable Group Theory for Chemists. Wiley.com.

Koohestani, K., 2013. A computational framework for the form-finding and design of tensegrity structures. Mechanics Research Communications 54, 41-49.

Kovacs, F., and Tarnai, T., 2009. Two-dimensional analysis of bar-and-joint assemblies on a sphere: Equilibrium, compatibility and stiffness. International Journal of Solids and Structures 46(6), 1317-1325.

Kuznetsov, E. N., 1991. Systems with infinitesimal mobility: Part I--Matrix analysis and first-order infinitesimal mobility. Journal of Applied Mechanics 58(2), 513-519.

Lu, J. Y., Luo, Y. Z., and Li, N., 2007. Mobility and equilibrium stability analysis of pin-jointed mechanisms with equilibrium matrix SVD. Journal of Zhejiang University-Science A 8(7), 1091-1100.

Macdonald, A. J., 2007. Structure and Architecture. Routledge.

Masic, M., Skelton, R. E., and Gill, P. E., 2005. Algebraic tensegrity form-finding. International Journal of Solids and Structures 42(16-17), 4833-4858.

Maxwell, J. C., 1864. On the calculation of the equilibrium and stiffness of frames. Philosophical Magazine 27, 294-299.

Murtha-Smith, E., 1988. Alternate path analysis of space trusses for progressive collapse. Journal of Structural Engineering 114(9), 1978-1999.

Ohsaki, M., and Zhang, J. Y., 2006. Stability conditions of prestressed pin-jointed structures. International Journal of Non-Linear Mechanics 41(10), 1109-1117.

Pellegrino, S., and Calladine, C. R., 1986. Matrix analysis of statically and kinematically indeterminate frameworks. International Journal of Solids and Structures 22(4), 409-428.

Sareh, P., and Guest, S. D., 2015a. Designing symmetric derivatives of the Miura-ori, Advances in Architectural Geometry 2014. Springer, pp. 233-241.

Sareh, P., and Guest, S. D., 2015b. A framework for the symmetric generalisation of the

Miura-ori. International Journal of Space Structures, Special Issue on Folds and Structures (in review).

Sebastian, W. M., 2004. Collapse considerations and electrical analogies for statically indeterminate structures. Journal of Structural Engineering 130(10), 1445-1453.

Sultan, C., 2013. Stiffness formulations and necessary and sufficient conditions for exponential stability of prestressable structures. International Journal of Solids and Structures 50(14-15), 2180-2195.

Sultan, C., Corless, M., and Skelton, R. E., 2001. The prestressability problem of tensegrity structures: some analytical solutions. International Journal of Solids and Structures 38(30-31), 5223-5252.

Tarnai, T., 1980. Simultaneous static and kinematic indeterminacy of space-trusses with cyclic symmetry. International Journal of Solids and Structures 16(4), 347-359.

Vassart, N., Laporte, R., and Motro, R., 2000. Determination of mechanism's order for kinematically and statically indetermined systems. International Journal of Solids and Structures 37(28), 3807-3839.

Wei, G. W., Chen, Y., and Dai, J. S., 2014. Synthesis, mobility and multifurcation of highly overconstrained deployable polyhedral mechanisms. Journal of Mechanical Design 136(9), 091003.

Wei, G. W., and Dai, J. S., 2014. A spatial eight-bar linkage and its association with the deployable platonic mechanisms. Journal of Mechanisms and Robotics 6(2), 021010.

Wei, G., and Dai, J. S., 2010. Mobility and geometric analysis of the Hoberman switch-pitch ball and its variant. Journal of Mechanisms and Robotics 2(3), 031010.

Zhang, J. Y., Guest, S. D., and Ohsaki, M., 2009. Symmetric prismatic tensegrity structures. Part I: Configuration and stability. International Journal of Solids and Structures 46(1), 1-14.

Zhang, P., Kawaguchi, K., and Feng, J., 2014. Prismatic tensegrity structures with additional cables: Integral symmetric states of self-stress and cable-controlled reconfiguration procedure. International Journal of Solids and Structures 51(25-26), 4294-4306.

Zhao, J. S., Chu, F. L., and Feng, Z. J., 2009. The mechanism theory and application of deployable structures based on SLE. Mechanism and Machine Theory 44(2), 324-335.

Zingoni, A., 2009. Group-theoretic exploitations of symmetry in computational solid and structural mechanics. International Journal for Numerical Methods in Engineering 79(3), 253-289.

Zingoni, A., 2014. Group-theoretic insights on the vibration of symmetric structures in engineering. Philosophical Transactions of the Royal Society A: Mathematical, Physical and Engineering Sciences 372(2008), 20120037.

List of table captions

List of figure captions

Fig. 1. A C_{2nv} symmetric pin-jointed structure (n=2): (a) top view; (b)3D view.

Fig. 2. Results for the C_{4v} symmetric structures with the same r_{d}: (a) minimum singular value; (b) second-smallest singular value.

Fig. 3. Results for the C_{16v} symmetric structures with the same r_{d}: (a) minimum singular value; (b) second-smallest singular value.

Fig. 4. Results for the C_{4v} symmetric structures with the same h: (a) the minimum singular value; (b) the second-smallest singular value

Fig. 5. Results for the C_{20v} symmetric structures with the same h: (a) the minimum singular value; (b) the second-smallest singular value.

Fig. 6. A C_{6v} symmetric structure with different nodal position deviations: (a) C_{3v}; (b) C_{2v}; (c) C_v.

Fig. 7. A C_{8v} structure with different nodal position deviations: (a) C_{4v} symmetric; (b) C_{2v} symmetric; (c) C_v symmetric.

Fig. 8. A 2D symmetric framework: (a) initial geometry; (b) removing one of the main diagonal elements; (c) removing one of the boundary elements; (d) removing one of the secondary diagonal elements.

Fig. 9. Typical configurations with six members removed: (a-b) C_{6v} symmetric; (c-d) C_{3v} symmetric; (e-f) C_{2v} symmetric; (g) C_3 symmetric; (h) C_v symmetric.

Fig. 10 A symmetric Kiewitt type structure: (a) 3D view; (b) plan view and mirror operations.

Fig. 11. Eleven independent configurations of the Kiewitt type symmetric structure with a single member removed: (a) the central vertical bar; (b) an inner vertical bar; (c) an outer vertical bar along the symmetric axis; (d) an outer vertical bar not along the symmetric axis; (e) an inner ring bar; (f) a top bar of the inner ring; (g) a top bar of the middle ring; (h) a top bar of the outer ring; (i) a bottom bar of the inner ring; (j) a bottom bar of the middle ring; (k) a bottom bar of the outer ring.

Fig. 12. Some typical configurations of the Kiewitt type structure with multiple members removed: (a) the central vertical bar; (b) the vertical bars of the inner ring; (c) the vertical bars of the outer ring; (d) the vertical bars of both the inner ring and the outer ring; (e) the inner ring bars; (f) the outer ring bars; (g) the inner and outer ring bars; (h) the radial bars of the outer ring.

Fig. 13. Symmetric frameworks: (a) 2D four-link structure; (b-c) 3D 21-bar assembly.

Fig. 14. The O_h symmetric structures: (a) pin-jointed structure; (b) over-constrained mechanism.

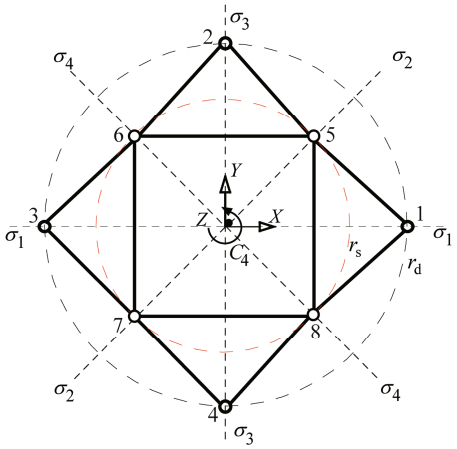

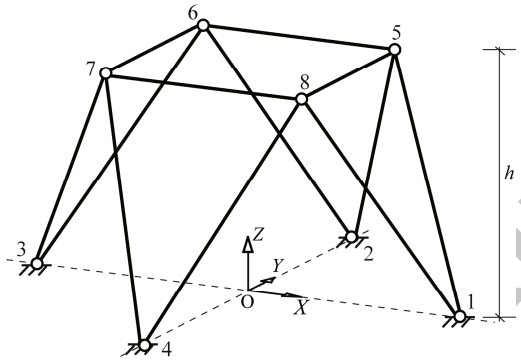

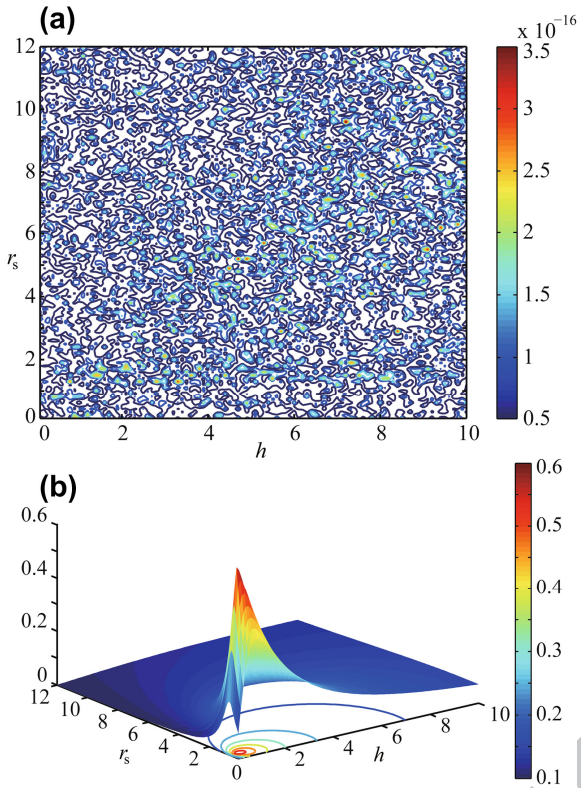

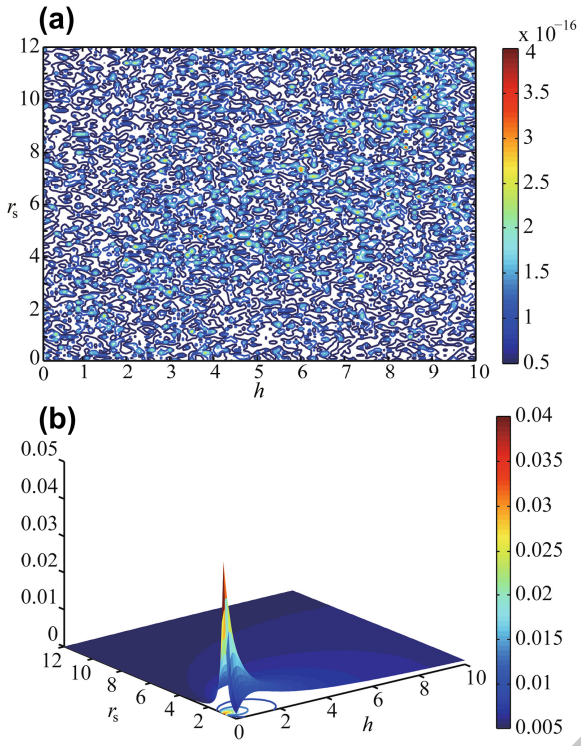

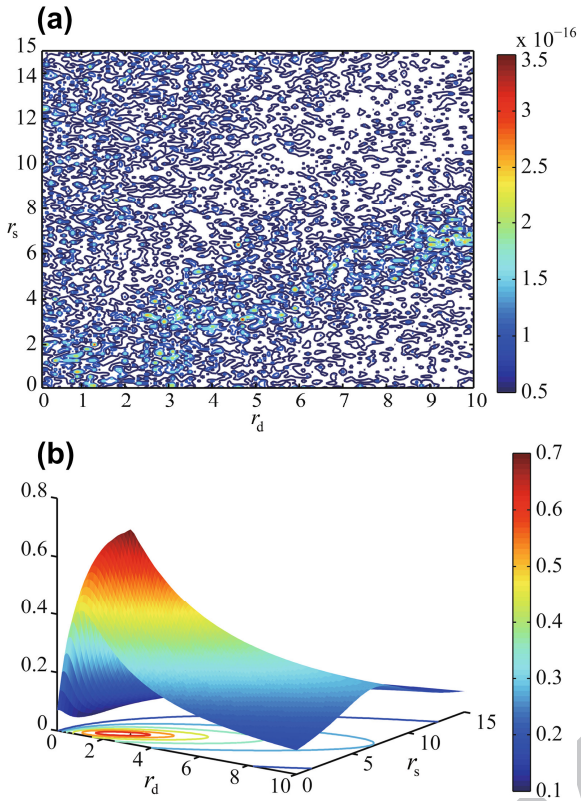

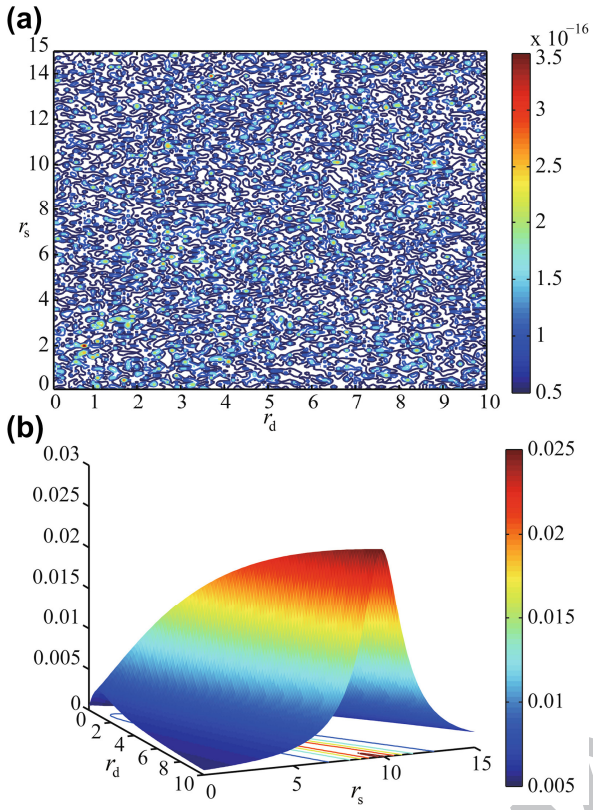

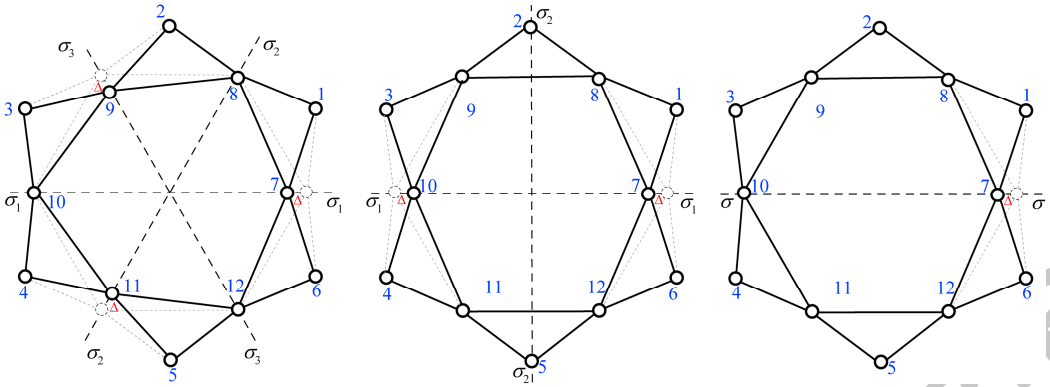

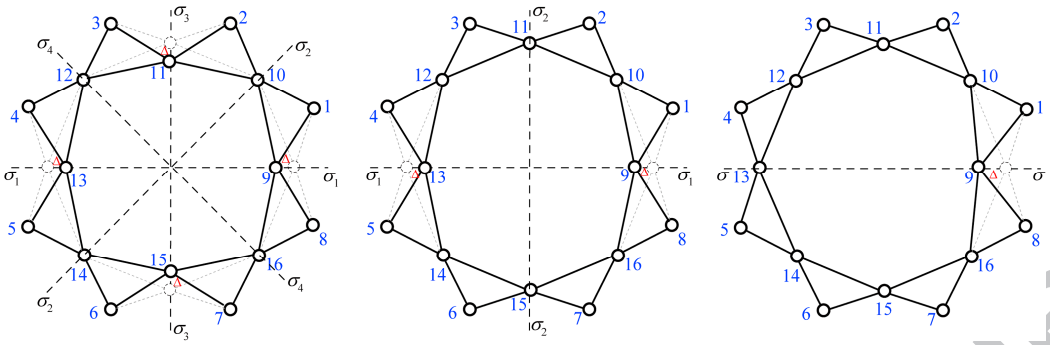

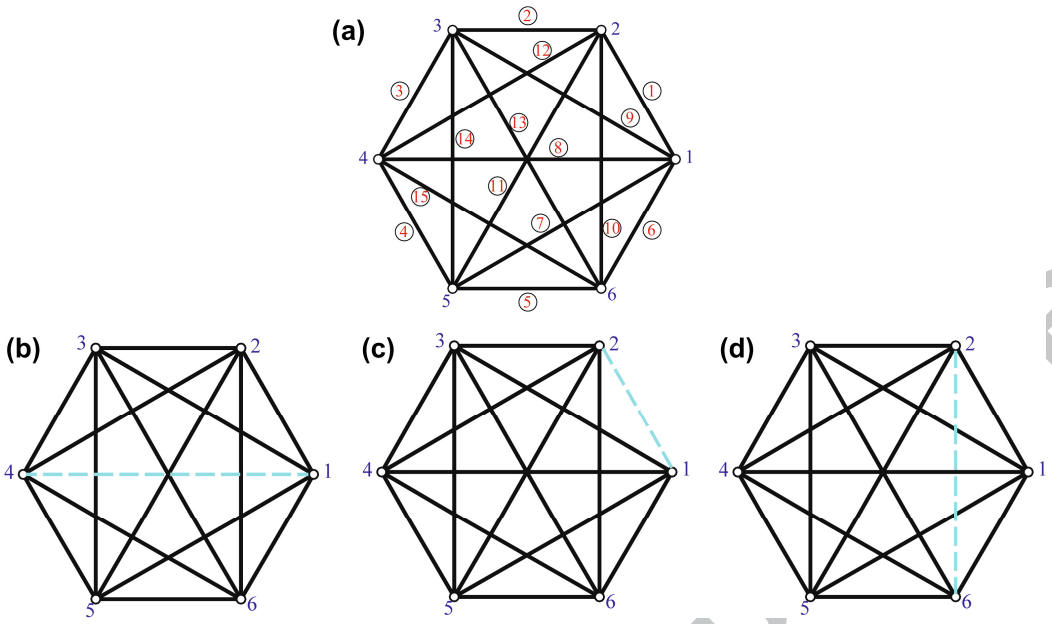

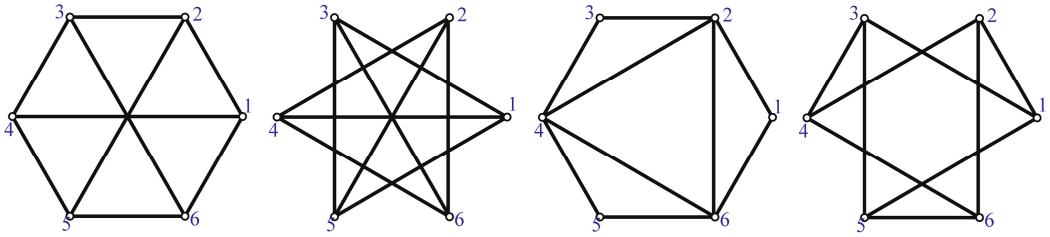

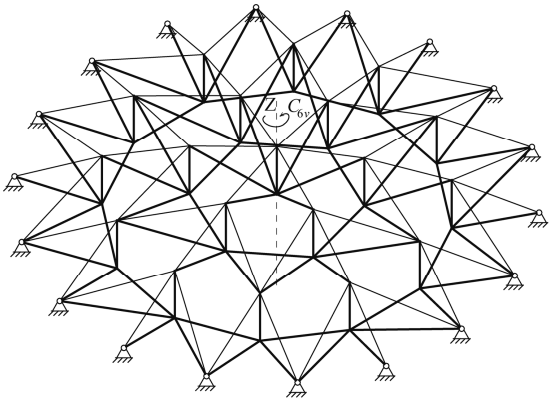

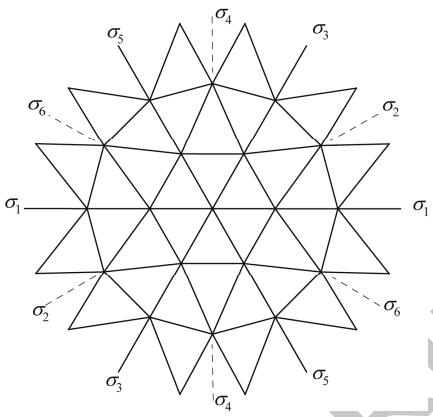

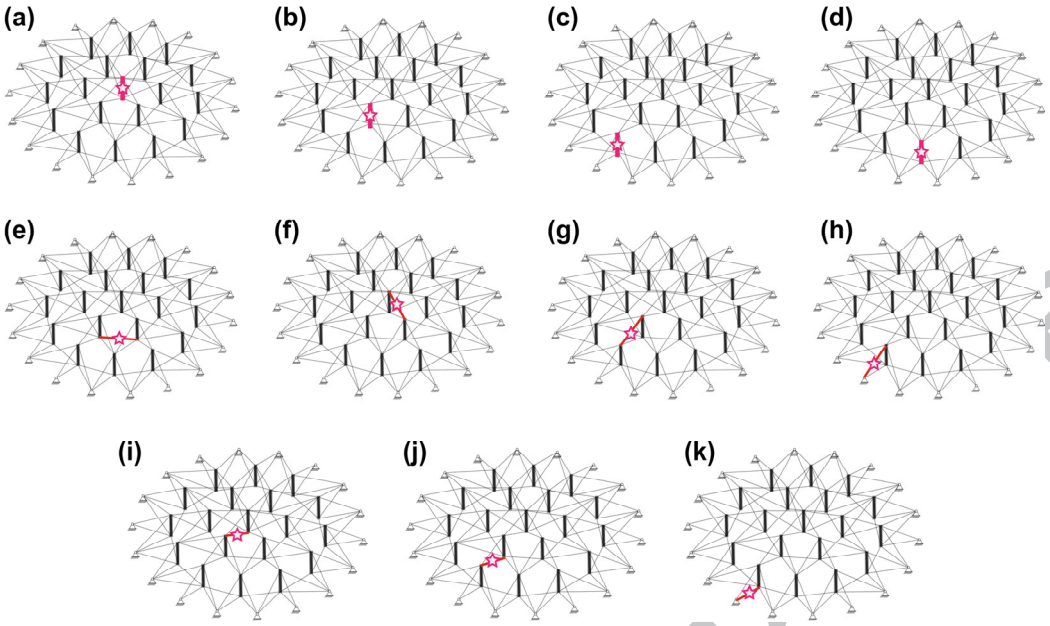

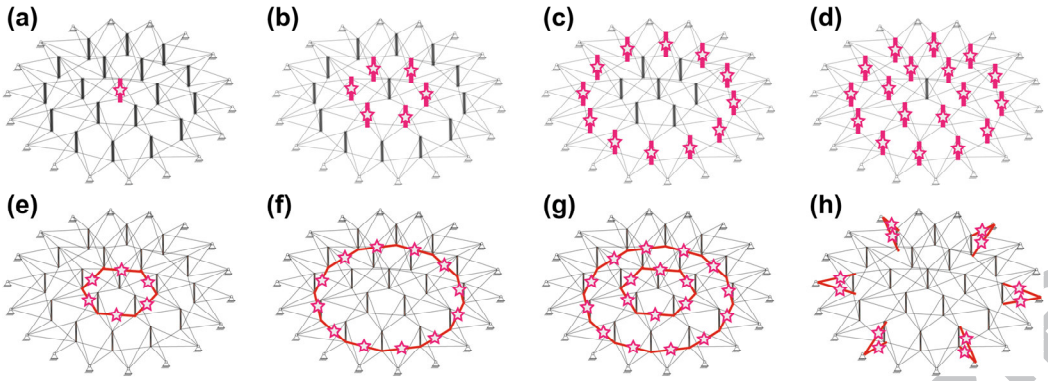

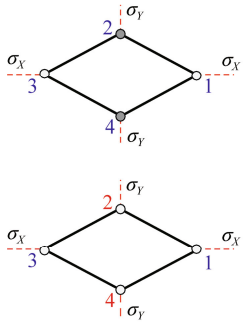

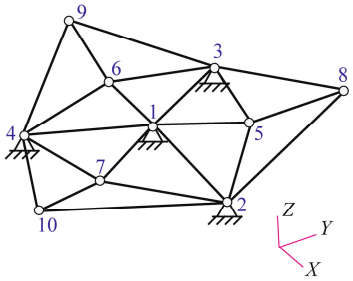

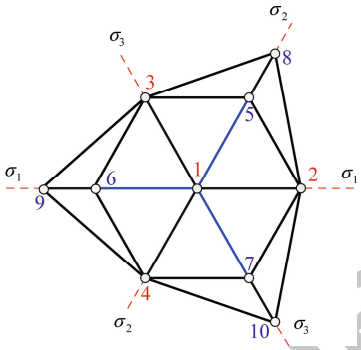

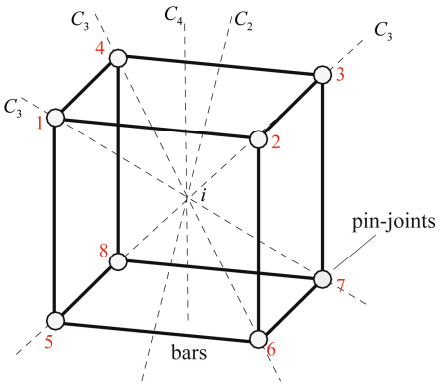

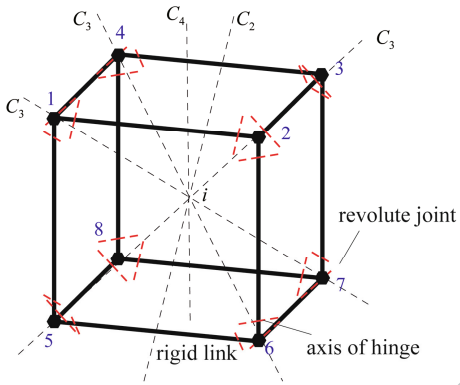

Table 1

Group C_{2nv}	E	$C_{2n}^{i}, i \in [1, 2n-1]$	$n\sigma_{2j}, j \in [1, n]$	$n\sigma_{2j-1}, j \in [1, n]$
$\Gamma(j)$	$2n$	0	2	0
$\Gamma(b)$	$6n$	0	0	2
Γ_k	0	0	0	0
$\Gamma(m)-\Gamma(s)$	0	0	2	–2

Table 2

Symmetry group	C_{6v}	C_{3v}	C_{2v}	C_v	C_6	C_3	C_2	C_1
$m=1,\ \Gamma(m)=B_1$	B_1	A_1	B_1	A_1	B	A	B	A
$s=1,\ \Gamma(s)=B_2$	B_2	A_2	B_2	A_2	B	A	B	A

Table 3

Symmetry group	C_{8v}	C_{4v}	C_{2v}	C_v	C_8	C_4	C_2	C_1
$m=1,\ \Gamma(m)=B_1$	B_1	A_1	A_1	A_1	B	A	A	A
$s=1,\ \Gamma(s)=B_2$	B_2	A_2	A_2	A_2	B	A	A	A

Table 4

Geometry	Symmetry	$\Delta\Gamma(b)$	$\Gamma(m)$, $\Gamma(s)$	m , s
Fig. 8(a)	C_{6v}	$\varnothing$	$\Gamma(m)=\varnothing,\ \Gamma(s)=2A_1+E_1+E_2$	$m=0,\ s=6$
Fig. 8(b)	C_{2v}	A_1	$\Gamma(m)=\varnothing,\ \Gamma(s)=2A_1+A_2+B_1+B_2$	$m=0, s=5$
Fig. 8(c)	C_v	A_1	$\Gamma(m)=\varnothing,\ \Gamma(s)=3A_1+2A_2$	$m=0,\ s=5$
Fig. 8(d)	C_v	A_1	$\Gamma(m)=\varnothing,\ \Gamma(s)=3A_1+2A_2$	$m=0,\ s=5$

Table 5

Geometry	Symmetry	$\Delta\Gamma(b)$	$\Gamma(m)$, $\Gamma(s)$	m, s
Initial	C_{6v}	$\varnothing$	$\Gamma(s)=2A_1+E_1+E_2$	$m=0$, $s=6$
Fig. 9(a)	C_{6v}	$A_1+B_2+E_1+E_2$	$\Gamma(m)=B_2$, $\Gamma(s)=A_1$	$m=s=1$
Fig. 9(b)	C_{6v}	$A_1+B_1+E_1+E_2$	$\Gamma(m)=B_1$, $\Gamma(s)=A_1$	$m=s=1$
Fig. 9(c)	C_{3v}	$2A_1+2E$	$\Gamma(m)=\Gamma(s)=\varnothing$	$m=s=0$
Fig. 9(d)	C_{3v}	$2A_1+2E$	$\Gamma(m)=\Gamma(s)=\varnothing$	$m=s=0$
Fig. 9(e)	C_{2v}	$2A_1+A_2+B_1+2B_2$	$\Gamma(m)=B_2$, $\Gamma(s)=A_1$	$m=s=1$
Fig. 9(f)	C_{2v}	$2A_1+A_2+B_1+2B_2$	$\Gamma(m)=B_2$, $\Gamma(s)=A_1$	$m=s=1$
Fig. 9(g)	C_3	$2A+2E$	$\Gamma(m)=\Gamma(s)=\varnothing$	$m=s=0$
Fig. 9(h)	C_v	$4A_1+2A_2$	$\Gamma(m)=\Gamma(s)=\varnothing$	$m=s=0$

Table 6

Geometry	Symmetry	$\Delta\Gamma(b)$	$\Gamma(m)$, $\Gamma(s)$	m, s
Initial	C_{6v}	$\varnothing$	$\Gamma(m)=\varnothing$, $\Gamma(s)=4A_1+A_2+5B_1+B_2+4E_1+6E_2$	$m=0$, $s=31$
Fig. 11(a)	C_{6v}	A_1	$\Gamma(m)=\varnothing$, $\Gamma(s)=3A_1+A_2+5B_1+B_2+4E_1+6E_2$	$m=0$, $s=30$
Fig. 11(b)	C_v	A_1	$\Gamma(m)=\varnothing$, $\Gamma(s)=18A_1+12A_2$	$m=0$, $s=30$
Fig. 11(c)	C_v	A_1	$\Gamma(m)=\varnothing$, $\Gamma(s)=18A_1+12A_2$	$m=0$, $s=30$
Fig. 11(d)	C_v	A_1	$\Gamma(m)=\varnothing$, $\Gamma(s)=14A_1+16A_2$	$m=0$, $s=30$
Fig. 11(e)	C_v	A_1	$\Gamma(m)=\varnothing$, $\Gamma(s)=14A_1+16A_2$	$m=0$, $s=30$
Fig. 11(f)	C_v	A_1	$\Gamma(m)=\varnothing$, $\Gamma(s)=18A_1+12A_2$	$m=0$, $s=30$
Fig. 11(g)	C_v	A_1	$\Gamma(m)=\varnothing$, $\Gamma(s)=18A_1+12A_2$	$m=0$, $s=30$
Fig. 11(h)	C_v	A_1	$\Gamma(m)=\varnothing$, $\Gamma(s)=18A_1+12A_2$	$m=0$, $s=30$
Fig. 11(i)	C_v	A_1	$\Gamma(m)=\varnothing$, $\Gamma(s)=18A_1+12A_2$	$m=0$, $s=30$
Fig. 11(j)	C_v	A_1	$\Gamma(m)=\varnothing$, $\Gamma(s)=18A_1+12A_2$	$m=0$, $s=30$
Fig. 11(k)	C_v	A_1	$\Gamma(m)=\varnothing$, $\Gamma(s)=18A_1+12A_2$	$m=0$, $s=30$

Table 7

Geometry	Symmetry	$\Delta\Gamma(b)$	$\Gamma(m)$, $\Gamma(s)$	m, s
Initial	C_{6v}	$\varnothing$	$\Gamma(m)=\varnothing$	$m=0$
			$\Gamma(s)=4A_1+A_2+5B_1+B_2+4E_1+6E_2$	$s=31$
Fig. 12(a)	C_{6v}	A_1	$\Gamma(m)=\varnothing$	$m=0$
			$\Gamma(s)=3A_1+A_2+5B_1+B_2+4E_1+6E_2$	$s=30$
Fig. 12(b)	C_{6v}	$A_1+B_1+E_1+E_2$	$\Gamma(m)=\varnothing$	$m=0$
			$\Gamma(s)=3A_1+A_2+4B_1+B_2+3E_1+5E_2$	$s=25$
Fig. 12(c)	C_{6v}	$2A_1+B_1+B_2+2E_1+2E_2$	$\Gamma(m)=\varnothing$	$m=0$
			$\Gamma(s)=2A_1+A_2+4B_1+2E_1+4E_2$	$s=19$
Fig. 12(d)	C_{6v}	$3A_1+2B_1+B_2+3E_1+3E_2$	$\Gamma(m)=\varnothing$	$m=0$
			$\Gamma(s)=A_1+A_2+3B_1+E_1+3E_2$	$s=13$
Fig. 12(e)	C_{6v}	$A_1+B_2+E_1+E_2$	$\Gamma(m)=\varnothing$	$m=0$
			$\Gamma(s)=3A_1+A_2+5B_1+3E_1+5E_2$	$s=25$
Fig. 12(f)	C_{6v}	$A_1+A_2+B_1+B_2+2E_1+2E_2$	$\Gamma(m)=\varnothing$	$m=0$
			$\Gamma(s)=3A_1+4B_1+2E_1+4E_2$	$s=19$
Fig. 12(g)	C_{6v}	$2A_1+A_2+B_1+2B_2+3E_1+3E_2$	$\Gamma(m)=B_2$	$m=1$
			$\Gamma(s)=2A_1+4B_1+E_1+3E_2$	$s=14$
Fig. 12(h)	C_{6v}	$2A_1+2B_1+2E_1+2E_2$	$\Gamma(m)=\varnothing$	$m=0$
			$\Gamma(s)=2A_1+A_2+3B_1+B_2+2E_1+4E_2$	$s=19$

Table 8

Group C_{2v}	Γ_T	Γ_R	$\Gamma(j)$	$\Gamma(b)$	Γ_k	$\Gamma(m)-\Gamma(s)$	$\Delta\Gamma_k$
E	2	1	4	4	2	−1	2
C_2	−2	1	0	0	0	1	0
σ_X	0	−1	2	0	2	1	0
σ_Y	0	−1	2	0	0	−1	2

Table 9

Group C_{3v}	Γ_T	$\Gamma(j)$	$\Gamma(b)$	Γ_k	$\Gamma(m)-\Gamma(s)$	$\Delta\Gamma_k$
E	3	10	21	12	−3	4
$2C_3$	0	1	0	0	0	1
3σ	1	4	3	2	−1	2

Table 10

Symmetry operations	E	$8C_3$	$6C_2$	$6C_4$	$3C_2$	i	$6S_4$	$8S_6$	$3\sigma_h$	$6\sigma_d$
$\Gamma(j)$	8	2	0	0	0	0	0	0	0	4
$\Gamma(b)$	12	0	2	0	0	0	0	0	4	2
Γ_k	6	0	–2	2	–2	0	0	0	0	0
$\Gamma(m)-\Gamma(s)$	6	0	0	–2	2	0	0	0	–4	2
$\Delta\Gamma_k$	12	0	2	0	0	0	0	0	–4	–2